Granular column collapse: Analysis of grain-size effects

Miguel Cabrera[*] and Nicolas Estrada[†]

Department of Civil and Environmental Engineering, Universidad de los Andes, Bogotá, Colombia

The column collapse experiment is a simplified version of the complex granular flows observed in both natural and industrial contexts. Due to its simple setup and rich behavior, the column collapse has been studied experimentally and numerically by several authors. The purpose of the analyses presented in this paper is to verify whether some of the results presented in these publications are affected by grain-size effects. In order to do so, we simulate two-dimensional granular columns by means of a discrete-element method, i.e., contact dynamics. Specifically, we study the influence of the grain size, as compared to the system size, on the resultant deposit geometry and collapse duration. We show that (i) some of the previously published results may be affected by grain-size effects, (ii) in order to avoid these effects, the system-size to grain-size ratio must be larger than 75 for short columns and larger than 50 for tall columns, and (iii) the quantities that are the most affected by grain-size effects are the column mobility and the collapse duration. Our findings serve as a tool for comparing results obtained by different researchers and draw guidelines on the number of grains that must be used in order to avoid grain-size effects.

I. INTRODUCTION

Granular column collapse can be seen as a simplified image of the complex dynamics observed in gravity-driven natural flows (e.g., landslides, debris flows, and rock avalanches) and manufactured systems (e.g., silos and channels used in the pharmaceutical and food industries). In this experiment, a granular assembly is built with an initial height H_0 and width R_0 and then allowed to collapse by self-weight onto a horizontal surface. The final runout R_f, deposit height H_f, and collapse duration T_f are the most commonly used measures in the description of collapse dynamics.

The use of the column collapse experiment to study granular materials was proposed simultaneously by Lube *et al.* [1] and Lajeunesse *et al.* [2]. Ever since, because of its easy setup and reproduction, the experiment has gained relevance and rapid acceptance within the granular media community, establishing it as a benchmark case for transitional granular flows in both dry [3–7] and submerged [8–11] conditions.

In general terms, previous studies present a unified description of the column collapse dynamics. However, the results presented in these studies differ slightly, even if the experiments were conducted in similar conditions. In order to illustrate this statement, let us consider the column mobility

$$R^* = \frac{R_f - R_0}{R_0}. \quad (1)$$

It is well known that R^* is highly dependent on the column aspect ratio $a = H_0/R_0$. Moreover, two regimes have been identified (i.e., short and tall columns) in which R^* scales differently with a,

$$R^* = \begin{cases} c_s a & \text{for } a < a^\dagger \\ c_t a^b & \text{for } a > a^\dagger, \end{cases} \quad (2)$$

where c_s, c_t, and b are fitting coefficients and $a^\dagger$ is the transition point between the two regimes. Table I presents the values for c_s, c_t, b, and $a^\dagger$ reported in ten different studies. Notable differences can be observed between studies conducted in similar conditions, especially for c_s, c_t, and $a^\dagger$. In addition, Table I presents the system-size to grain-size ratio R_0/d, where d is the mean diameter of the grains. Some values of R_0/d are as low as 8, which is close to well known length scales such as the thickness of shear bands or the length of force chains (i.e., approximately $10d$) [19–22]. Thus, it is reasonable to hypothesize that some of the studied systems are too small, in terms of the number of particles, and that the reported results can be influenced by grain-size effects.

In this work we carry out a systematic study of the collapse of two-dimensional granular columns, focusing on the influence of the grains size, as compared to the system size. Specifically, we attempt to answer the following questions.

(i) What is the minimum system-size to grain-size ratio that the columns should have in order to avoid significant grain-size effects?

(ii) What are the effects of this ratio on the deposit geometry and the collapse duration?

In order to approach these questions, we use the contact dynamics method to simulate the collapse of a series of columns with varying aspect ratio a and system-size to grain-size ratio R_0/d. Then we analyze the effects of these variables on the column mobility R^*, final height H_f, and collapse duration T_f.

We present the numerical methods and the simulation details in Sec. II. In Sec. III we present our results. In Sec. IV we summarize and discuss our findings.

---
[*]ma.cabrera140@uniandes.edu.co
[†]n.estrada22@uniandes.edu.co

TABLE I. Previous results for dry experiments (Expt.) or numerical simulations (Num.) of the granular column collapse. Here R_0/d is the system-size to grain-size ratio; c_s, c_t, and b are the fitting coefficients in Eq. (2); and $a^\dagger$ is the transition point that differentiates the regimes of short and tall columns.

Source	Setup	R_0/d	c_s	c_t	b	$a^\dagger$
Ref. [1]	Expt. axisymmetric	[12.7–303]	1.24	1.60	0.50	1.7
Ref. [2]	Expt. axisymmetric	[37.1–201.4]	1.35	2.0	0.50	0.74
Ref. [12]	Expt. quasi-two-dimensional	[20–200]			0.65	
Ref. [13]	Expt. quasi-two-dimensional	[13–83.3]	1.2	1.9	0.66	2.3
Ref. [14]	Num. two-dimensional	[10–40]	2.5	3.25	0.70	2.0
Ref. [15]	Num. two-dimensional					[0.39–0.49]
Ref. [3]	Expt. quasi-two-dimensional	[16.6–47]	0.8	[1.0–1.3]	0.70	2.0
Ref. [16]	Num. two-dimensional	[10–45]	[2.4–6.9]	[2.8–8.6]	0.70	⌣2.5
Ref. [17]	Expt. Planar two-dimensional	[8–16]			[0.72, 0.81]	⌣(2.5, 4.1)
Ref. [18]	Expt. Axisymetric	[28–107]	1.29	1.34	0.66	1.75

II. METHODS

A. Contact dynamics

The simulations were carried out by means of the contact dynamics method, developed by Moreau and Jean [23–26]. This discrete-element method can be understood as a combination of three main ingredients. The first ingredient is the set of equations of motion, which, integrated over a small time step, relate the impulse to the change of momentum of each particle over the time step. The second ingredient is a set of contact laws which relate the impulses exerted at each contact with the change of relative velocity during the time step. The method supposes that grains are perfectly rigid, and the usual contact laws are perfect volume exclusion and Coulomb friction. The third ingredient of the method is an algorithm of solution. Since the system of equations to be solved is implicit, the impulses and changes of momentum of each grain are determined using an iterative algorithm similar to a Gauss-Seidel scheme. Finally, these impulses and changes of momentum are used to calculate the contact forces and grain positions at the end of the time step. For a detailed description of the contact dynamics method, see [27,28].

Because of the nonsmooth formulation of both the equations of motion and the contact laws, the contact dynamics method allows larger time steps than more conventional Discrete Element Method algorithms such as molecular dynamics [29]. In addition, since the contact laws do not need to be regularized, the method requires fewer contact parameters; this eases the method's use and calibration. As limitations, the method cannot be used to investigate phenomena that depend on the particle's stiffness and the algorithm is difficult to parallelize because of its implicit nature. Nevertheless, similar results can be obtained with both contact dynamics and molecular dynamics for stiff particles [30].

B. Column construction

The samples were composed of disks with density $\rho = 2600$ kg/m^3. The grain diameters were uniformly distributed between d_{min} and d_{max}, with $d_{max} = 0.001$ m and $d_{max}/d_{min} = 3/2$. These grains were randomly placed in the nodes of a square grid; the separation between nodes was $1.1 d_{max}$, in order for the grains not to touch or overlap. Finally, the grains were placed inside a rectangular box with fixed and frictionless walls.

In order to densify the samples, a horizontal gravity field was imposed [i.e., $\vec{g} = (-10, 0)$ m/s^2]. As a result, a granular column formed in the left side of the box. The initial shape of this column was described in terms of its width R_0 and height H_0. The system-size to grain-size ratio R_0/d varied between 10 and 200 and the aspect ratio a varied between 0.25 and 16. Consequently, the number of grains used in each column varied between $\mathcal{O}^2$ and $\mathcal{O}^5$.

C. Column collapse

In order to conduct the collapse experiment, a vertical gravity field was imposed [i.e., $\vec{g} = (0, -10)$ m/s^2]. During the collapse phase, the friction and restitution coefficients were $\mu = 1$ and $e = 0.5$, respectively; these contact parameters are the same as those employed by Staron and Hinch [14]. The friction coefficient of the base was $\mu = 1$ and the lateral walls were frictionless.

Figures 1 and 2 show the typical evolution of the collapse for a short and a tall column, respectively. Three stages can be distinguished. First, the grains fall vertically. For short columns, the only particles that fall are those in the free face of the column. Second, the falling particles transition to a lateral spreading movement. Third, particles decelerate while the lateral spreading reduces to a superficial flow prior to the system's final deposition.

The shape of the final deposit was described in terms of its runout R_f and height H_f. The collapse duration T_f was the time at which the total number of contacts N_c stagnated to a constant value [i.e., points (g) and (f) in the insets of Figs. 1 and 2, respectively].

III. RESULTS

The following sections present our results on the effect of the system-size to grain-size ratio R_0/d on two characteristics: the final deposit geometry and the collapse duration.

A. Effects on the final deposit geometry

As explained in the Introduction, one of the measures that is commonly used to describe the final deposit geometry is
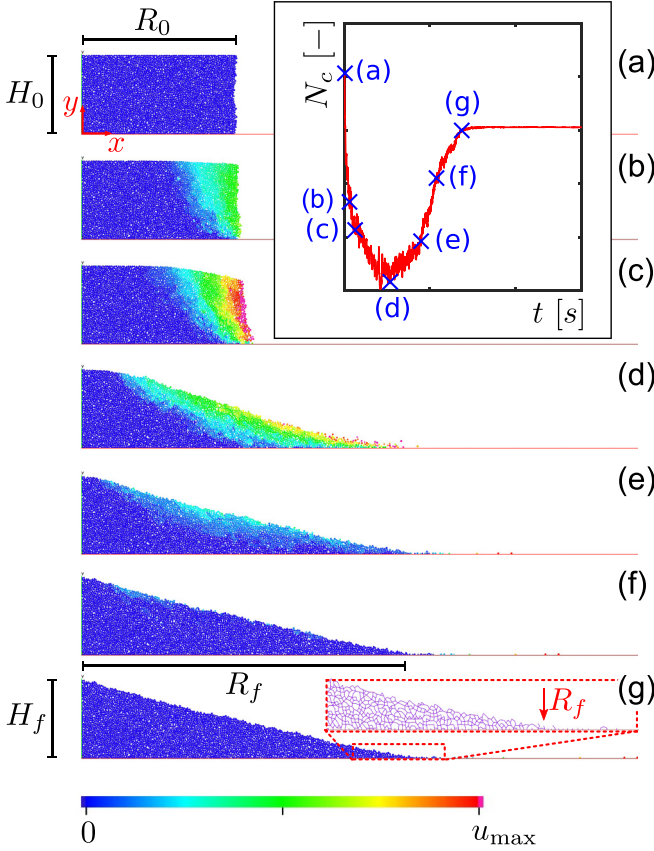
FIG. 1. Collapse of a short granular column ($a = 0.5$ and $R_0/d = 75$). Three stages can be distinguished: (b) Initially, the free face of the column falls almost vertically; (c) and (d) the falling grains transition to a lateral spreading movement; (e)–(g) finally, the system comes to rest with a thin surface flow. As shown in (g) R_f was the width of the deposit contact network. The inset shows the evolution of the number of contacts N_c as a function of time.
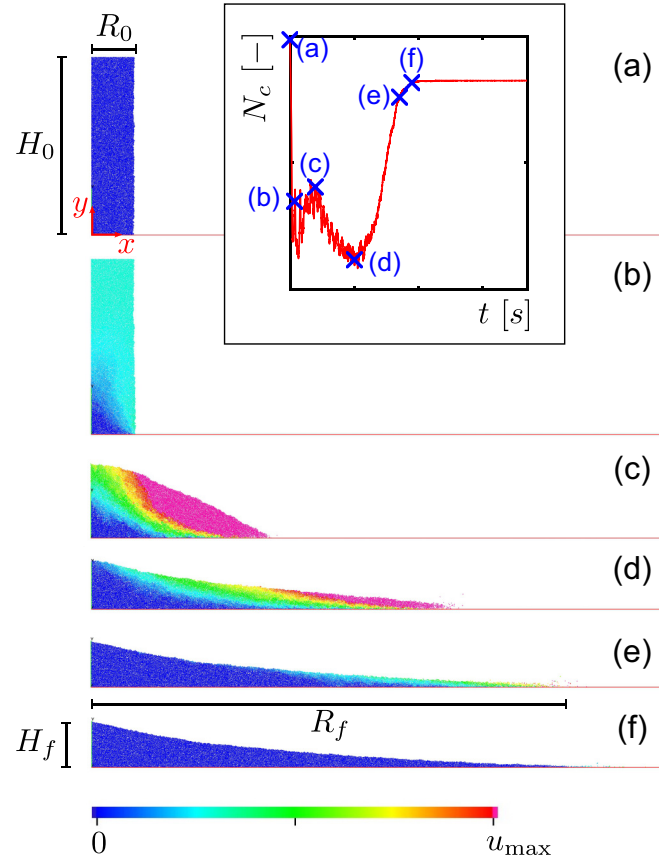

FIG. 2. Collapse of a tall granular column ($a = 4$ and $R_0/d = 50$). Three stages can be distinguished: (b) Initially, the column falls almost vertically; (c) and (d) the falling grains transition to a lateral spreading movement; (e) and (f) finally, the system comes to rest with a thin surface flow. The inset shows the evolution of the number of contacts N_c as a function of time.

the column mobility R^*. Figure 3(a) shows R^* as a function of the system-size to grain-size ratio R_0/d for different values of the initial column aspect ratio a. First, it can be seen that R^* increases with a, which means that a taller column will have greater mobility. Second, it can be seen that R^* initially increases with R_0/d and then stagnates to an approximately constant value. This clearly shows the influence of the grains size as compared to the system size. In other words, in order to avoid grain-size effects, the column's width R_0 must be larger than a certain number of grains. According to our simulations, this number of grains is close to 75 for short columns and close to 50 for tall columns. This coincides with the experimental results found by Warnett *et al.* [18]. Figure 3(b) shows the relative error of R^*, estimated as $(R^*_{max} - R^*)/R^*_{max}$, where R^*_{max} is the mobility for the largest R_0/d reached for each a. For example, for columns with R_0/d close to 20, the relative error in R^* can be as large as 40%.

In order to identify the transition between the regimes of short and tall columns, it is useful to represent R^* as a function of a. Figure 4(a) shows R^* as a function of a for different values of R_0/d. Again, it can be seen that R^* increases with both a and R_0/d and it saturates for large values of R_0/d. In addition, Fig. 4(a) allows for identifying the transition point

$a^\dagger$, which differentiates the regimes of short and tall columns. The fitting for these regimes, in the form of Eq. (2), leads to the following scaling:

$$R^* \approx \begin{cases} 3.14a & \text{for } a < 2.38 \\ 3.73a^{0.8} & \text{for } a > 2.38. \end{cases} \quad (3)$$

In this equation, $c_s = 3.14$, $c_t = 3.73$, $b = 0.8$, and $a^\dagger = 2.38$ are the fitting coefficients for the largest R_0/d ratios reached for each a. Furthermore, Fig. 4(b) shows the evolution of these coefficients as functions of R_0/d. Note that c_s, c_t, and $a^\dagger$ are sensitive to changes in R_0/d and tend to stabilize as the system-size to grain-size ratio increases.

A second descriptor of the deposit geometry is its height H_f. Figure 5 shows the normalized height H_f/H_0, where H_0 is the initial height, as a function of a. First, this representation reveals a regime of very short columns (i.e., approximately for $a < 0.65$), for which the final deposits present a trapezoidal shape, preserving the initial height. Second, for columns with $a > 0.65$, the final deposits present a triangular shape and H_f/H_0 decreases as a power law of a. Third, H_f/H_0 is independent of R_0/d, meaning that the deposit height is not affected by grain-size effects. This can be summarized as
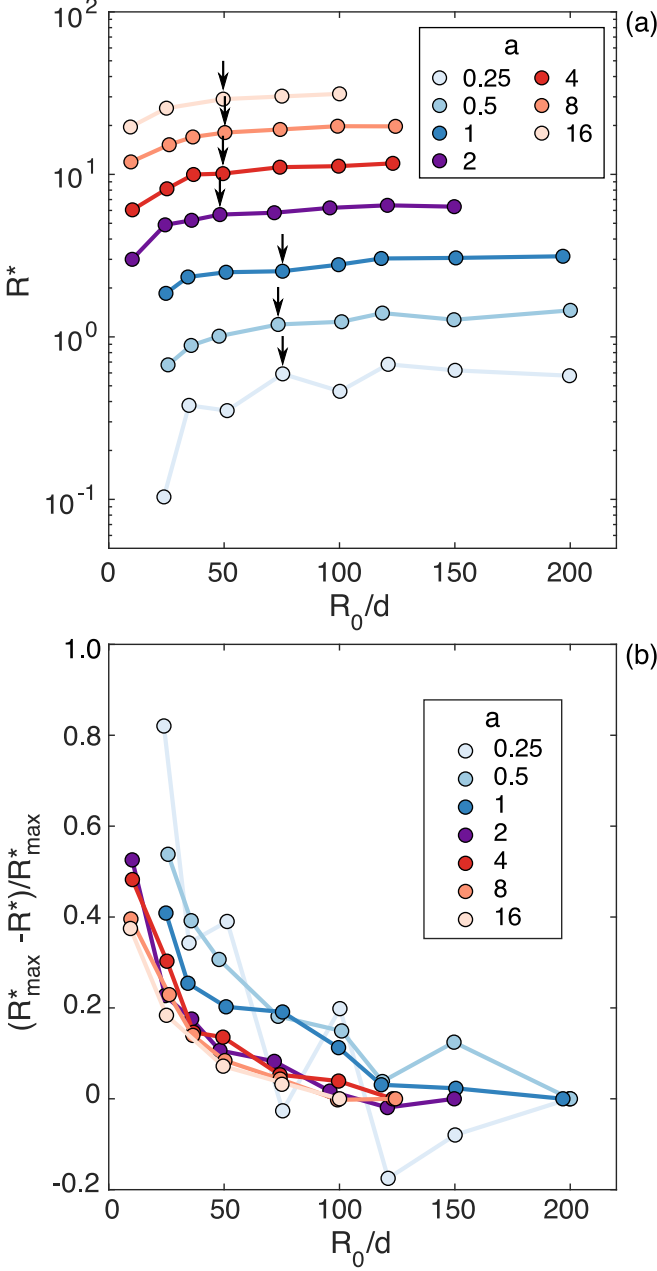
FIG. 3. (a) Column mobility R^* as a function of the system-size to grain-size ratio R_0/d and the initial aspect ratio a. (b) Relative error of R^* as a function of R_0/d. Here $R^*_{\max}$ is the mobility for the largest R_0/d reached for each a.

FIG. 4. (a) Column mobility R^* as a function of initial aspect ratio a and system-size to grain-size ratio R_0/d. The solid lines show the regimes of short and tall columns for the largest R_0/d analyzed in this work [i.e., Eq. (3)]. (b) Fitting coefficients for short and tall columns as a function of R_0/d. The dashed lines represent the coefficients obtained considering the largest R_0/d at each a, while the markers are computed for common values of R_0/d.

follows:

$$\frac{H_f}{H_0} \approx \begin{cases} 1 & \text{for } a < 0.65 \\ 0.72a^{-0.77} & \text{for } a > 0.65. \end{cases} \quad (4)$$

B. Effects on the collapse duration

A third descriptor of column collapse is the elapsed time between the column release and its final deposition T_f. Several authors have pointed out the difficulty in defining T_f precisely. Experimentally, T_f is defined as the instant at which the moving front reaches the final runout R_f, or a fraction of it [1,2,31]. The numerical approach makes the determination
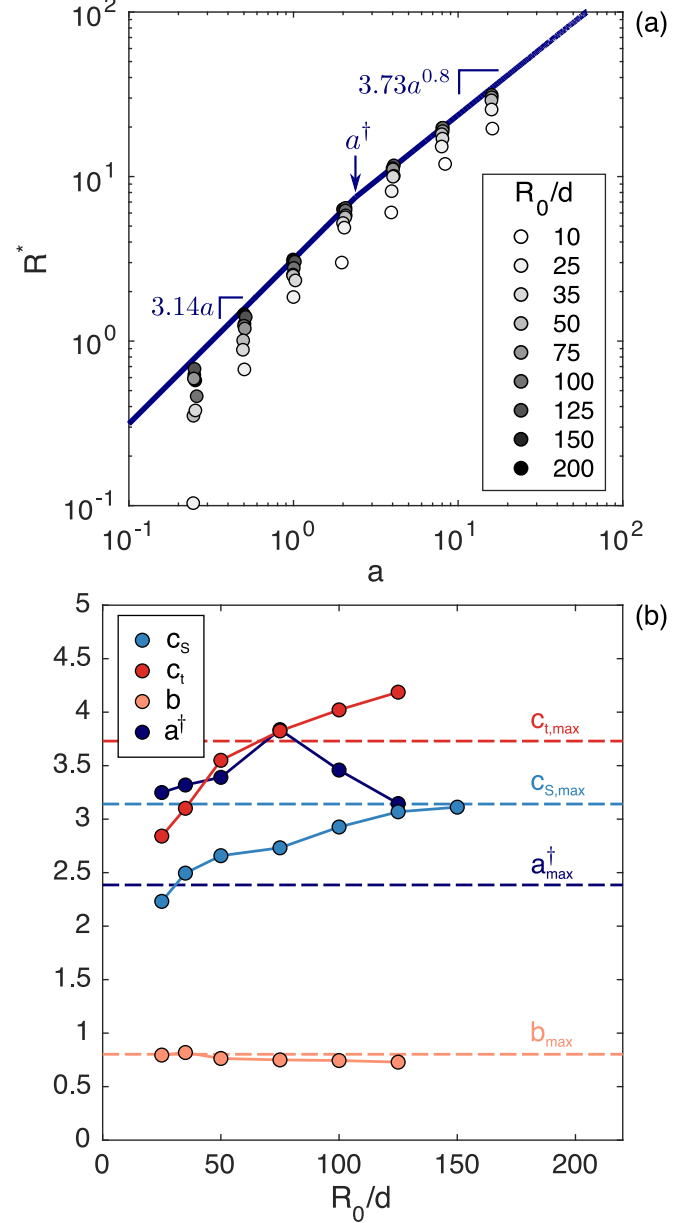
of T_f easier, taking advantage of the additional information on the granular system. Staron and Hinch measured T_f as the time at which sideways propagation stops and the full granular system comes to rest [14]. We used a similar strategy, based on the evolution of the number of contacts N_c during the column collapse.

Figure 6 present the evolution of N_c in time t for a short and a tall column and for different values of the system-size to grain-size ratio R_0/d. The number of contacts N_c is normalized by the initial value N_c^0, and time is normalized by
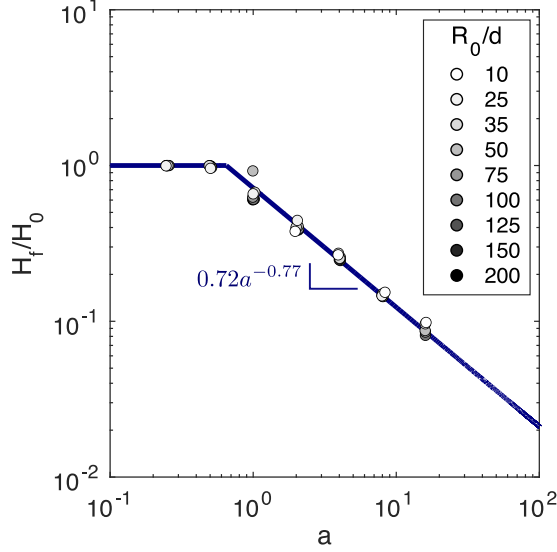
FIG. 5. Normalized deposit height H_f/H_0 as a function of the initial aspect ratio a and the system-size to grain-size ratio R_0/d.

the free-fall time:

$$T_0 = (2H_0/g)^{0.5}. \tag{5}$$

These figures show that the connectivity is partially lost at the initial stages and then partially regained during flow and deposition. In most cases, more than 90% of the initial number of contacts is recovered. Moreover, it can be seen that oscillations in N_c decrease with R_0/d, evincing a smaller influence of grain-size effects in the system behavior.

The time evolution of N_c also provides insight into the transitional flow stages (e.g., free fall, lateral spreading, and deposition). Figure 6(a) presents the case of short columns where no free fall is expected and N_c directly drops until reaching a minimum at the spreading phase; then the contact network builds up during deposition until reaching a stagnant value. In contrast, tall columns present three stages of collapse [see Fig. 6(b)]. During free fall, N_c rapidly drops after release and then slightly increases. Then, in the second stage, the number of contacts decreases as the overall motion transforms into lateral spreading, reaching a local minimum. Finally, while the lateral spreading decelerates, the deposit contact network builds up, reaching a stagnant value.

As for the column mobility, the collapse duration T_f can be related to the aspect ratio a. Figure 7 shows the normalized collapse duration T_f/T_0 as a function of the aspect ratio a for different values of the system-size to grain-size ratio R_0/d. It can be seen that T_f/T_0 is highly dependent on R_0/d in the regime of short columns, but T_f/T_0 is independent of R_0/d in the regime of tall columns. Moreover, for tall columns, T_f/T_0 decreases as a power law:

$$\frac{T_f}{T_0} \approx 3.9a^{-0.8}. \tag{6}$$

Figure 8 shows the relation between T_f and T_0 normalized by the characteristic time $(d/g)^{0.5}$. Again, it can be seen that for tall columns T_f can be estimated as a function of T_0: $T_f \approx 3.9a^{-0.8}T_0$. This is similar to the expression proposed
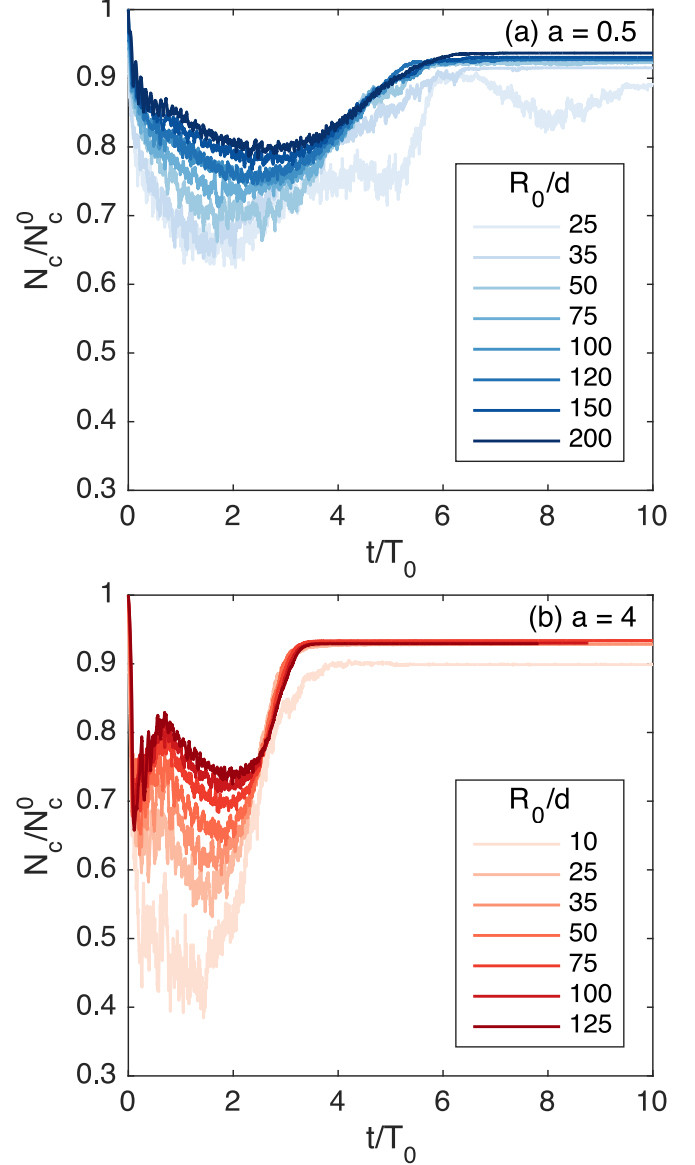

FIG. 6. Normalized number of contacts N_c/N_c^0 as a function of the normalized time t/T_0 for different values of the system-size to grain-size ratio R_0/d for (a) a short column (i.e., $a = 0.5$) and (b) a tall column (i.e., $a = 4$). The collapse duration T_f is computed as the point at which the system reaches a constant value of N_c.

in Ref. [14] ($T_f \approx 2.25T_0$) if one sets $a = 2$. Moreover, by combining Eqs. (5) and (6), T_f can be written as a function of R_0/d:

$$\frac{T_f}{(d/g)^{0.5}} \approx 5.5a^{-0.3}\left(\frac{R_0}{d}\right)^{0.5}. \tag{7}$$

IV. SUMMARY AND DISCUSSION

This paper presented a systematic study of the collapse of two-dimensional granular columns, focusing on the influence of grains size, as compared to system size. The aim of this work was twofold. First, we looked at the minimum system-size to grain-size ratio that the columns should have in order to avoid significant grain-size effects. Second, we assessed to
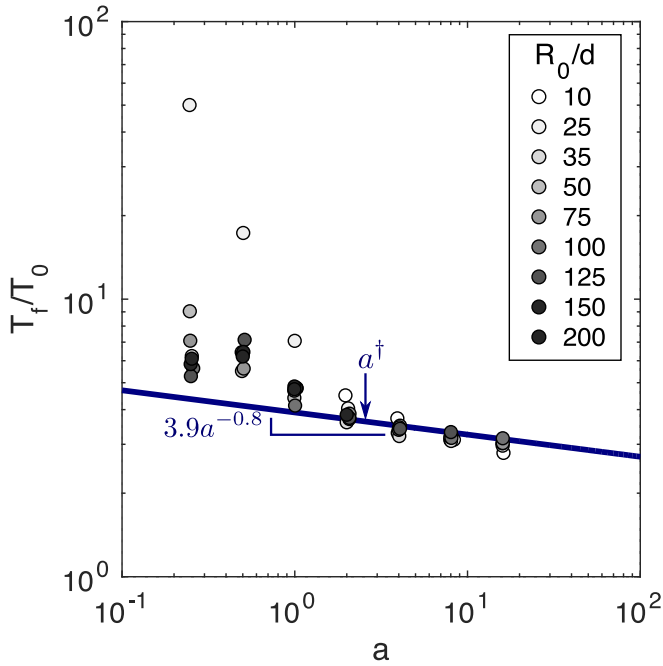
FIG. 7. Normalized collapse duration T_f/T_0 as a function of the aspect ratio a for different values of the system-size to grain-size ratio R_0/d. The solid line corresponds to Eq. (6).
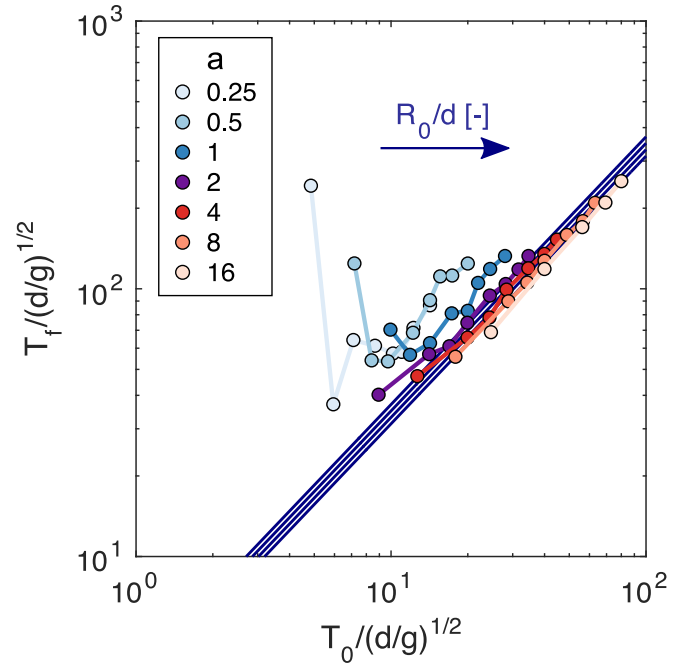

FIG. 8. Total collapse duration T_f as a function of the free-fall time $T_0 = (2H_0/g)^{0.5}$ normalized by the characteristic time $(d/g)^{0.5}$. The solid lines correspond to Eq. (7) for $a = 2, 4, 8,$ and 16.

what extent these effects are reflected on the deposit geometry and collapse duration. The numerical experiments were conducted on columns composed of two-dimensional disks of a common particle size through all simulations. The influence of grain size was investigated as a function of the system-size to grain-size ratio, relating the initial column width with the mean particle diameter. This size ratio varied between 10 and 200, for a range of column aspect ratios between 0.25 and 16.

First, we found that, in order to avoid significant grain-size effects, the system-size to grain-size ratio must be larger than 75 for short columns and larger than 50 for tall columns. This finding coincides with that of Warnett *et al.* for three-dimensional axisymmetric columns [18]. They found experimentally that grain-size effects vanish for system-size to grain-size ratios that are larger than 70 and 50, respectively. This suggests that most of the reference studies presented in Table I combine observations on columns where the grain size plays a significant role. For example, the small values of c_s and c_t found in [3,13] as well as the large values of $a^\dagger$ found in [17] could be the consequence of using columns of small system-size to grain-size ratio.

Second, we found that the measurements that are the most affected by grain-size effects are the column mobility and the collapse duration. In particular, we observed that using systems with an insufficient number of grains will decrease the column mobility and increase the collapse duration, especially for short columns. Curiously, the final column height was not affected by grain-size effects. These findings also coincide with the results found by Warnett *et al.* [18].

Further research on grain-size effects on granular columns may point to the study of polydisperse systems, focusing on the interplay between small and large grains in equivalent sets of particle-size distributions. The observations presented in this paper could prove beneficial in the interpretation of granular column experiments on saturated and submerged conditions.

[1] G. Lube, H. E. Huppert, R. S. J. Sparks, and M. A. Hallworth, J. Fluid Mech. **508**, 175 (2004).

[2] E. Lajeunesse, A. Mangeney-Castelnau, and J. P. Vilotte, Phys. Fluids **16**, 2371 (2004).

[3] C. Mériaux, Phys. Fluids **18**, 093301 (2006).

[4] L. Girolami, T. H. Druitt, O. Roche, and Z. Khrabrykh, J. Geophys. Res.: Solid Earth **113**, B02202 (2008).

[5] M. Trepanier and S. V. Franklin, Phys. Rev. E **82**, 011308 (2010).

[6] M. Farin, Experimental studies of the dynamics and of the seismic emission of gravitational instabilities, Ph.D. thesis, Institut de Physique du Globe de Paris, 2015.

[7] G. Pinzon and M. A. Cabrera, in *Proceedings of China-Europe Conference on Geotechnical Engineering*, edited by I. W. Wu

and H.-S. Yu, Springer Series in Geomechanics and Geoengineering Vol. 1 (Springer, Cham, 2018), pp. 591–596.

[8] C. Cassar, M. Nicolas, and O. Pouliquen, Phys. Fluids **17**, 103301 (2005).

[9] E. L. Thompson and H. E. Huppert, J. Fluid Mech. **575**, 177 (2007).

[10] O. Roche, S. Montserrat, Y. Niño, and A. Tamburrino, J. Geophys. Res.: Solid Earth **113**, B12203 (2008).

[11] A. Bougouin, L. Lacaze, and T. Bonometti, J. Fluid Mech. **826**, 918 (2017).

[12] N. J. Balmforth and R. R. Kerswell, J. Fluid Mech. **538**, 399 (2005).

[13] G. Lube, H. E. Huppert, R. S. J. Sparks, and A. Freundt, Phys. Rev. E **72**, 041301 (2005).

[14] L. Staron and E. J. Hinch, J. Fluid Mech. **545**, 1 (2005).

[15] R. Zenit, Phys. Fluids **17**, 031703 (2005).

[16] L. Staron and E. J. Hinch, Granular Matter **9**, 205 (2006).

[17] L. Lacaze, J. C. Phillips, and R. R. Kerswell, Phys. Fluids **20**, 063302 (2008).

[18] J. M. Warnett, P. Denissenko, P. J. Thomas, E. Kiraci, and M. A. Williams, Granular Matter **16**, 115 (2014).

[19] H. Mühlhaus and I. Vardoulakis, Geotechnique **37**, 271 (1987).

[20] J. F. Peters, M. Muthuswamy, J. Wibowo, and A. Tordesillas, Phys. Rev. E **72**, 041307 (2005).

[21] A. Tordesillas, D. M. Walker, and Q. Lin, Phys. Rev. E **81**, 011302 (2010).

[22] B. Andreotti, Y. Forterre, and O. Pouliquen, *Granular Media: Between Fluid and Solid* (Cambridge University Press, Cambridge, 2013).

[23] J. J. Moreau, Eur. J. Mech. A Solids **13**, 93 (1994).

[24] M. Jean, in *Mechanics of Geometrical Interfaces*, edited by A. P. S. Selvadurai and M. J. Boulon (Elsevier, Amsterdam, 1995).

[25] M. Jean, Comput. Methods Appl. Mech. Eng. **177**, 235 (1999).

[26] M. Jean, in *Micromécanique des Matériaux Granulaires*, edited by B. Cambou and M. Jean (Hermes, Paris, 2001), Chap. 4, pp. 199–324.

[27] F. Radjai and V. Richefeu, Mech. Mater. **41**, 715 (2009).

[28] *Discrete Numerical Modeling of Granular Materials*, edited by F. Radjaï and F. Dubois (Wiley-ISTE, New York, 2011).

[29] P. Cundall and O. Strack, Geotechnique **29**, 47 (1979).

[30] F. Radjai, J. Schäfer, S. Dipple, and D. Wolf, J. Phys. (France) I **7**, 1053 (1997).

[31] L. Rondon, O. Pouliquen, and P. Aussillous, Phys. Fluids **23**, 073301 (2011).